Current Pattern and Gas Flow Stabilization in Pulsed Plasma Accelerators

ALAN C. ECKBRETH*
United Aircraft Research Laboratories, E. Hartford, Conn.
AND
ROBERT G. JAHN†
Princeton University, Princeton, N. J.

Current sheets propagating in a parallel-plate accelerator are found to arrest their motion at an electrode-insulator junction, and there to lapse into stable, quasi-steady discharges. Kerr-cell photography, magnetic and electric probing, and terminal voltage measurements indicate that these stabilized discharges accelerate gas through themselves as long as gas from the prefilling of the discharge chamber is available, after which enhanced erosion of insulator and electrode material appears. To supply fresh gas to the stabilized current zone with a minimum of delay, a shock-tube gas injection technique is used. Even with this procedure, it is found that the current must be driven for hundreds of microseconds before a quasi-steady gas flow can be established in contrast to the tens of microseconds required for electrodynamic stabilization. This quasi-steady flow mode, characterized by both current pattern and gas flow stabilization again is observed to provide substantial acceleration of the inlet flow.

I. Introduction

TWO phases of stabilization have been identified in pulsed plasma accelerators: 1) current pattern stabilization, in which formerly convecting current distributions cease to propagate,[1-3] and 2) gas flow stabilization, wherein an externally supplied gas flow achieves a steady acceleration profile through the stabilized current pattern.[4,5] These stabilization processes are of interest in pulsed plasma accelerators both because of the fundamental questions they pose and because of their practical implementations. For example, one may inquire about the effect of current pattern stabilization on the plasma ejection losses of a pulsed accelerator, or about the details of the plasma acceleration process in a quasi-steady plasma accelerator, i.e., an accelerator in which both current pattern and gas flow stabilization coexist. On the other hand, one may employ such a quasi-steady accelerator to simulate a high-power, steady electromagnetic thruster, such as a magnetoplasmadynamic arc, for a short time. In this way one may, using transient instrumentation techniques, perform detailed interior diagnostic studies on the arc-accelerator environment which in the steady state would be too hostile for probing. Finally, operation of an accelerator in the quasi-steady mode is of interest in its own right since this may be the regime in which electromagnetic acceleration processes are optimized. The quasi-steady mode shares many of the advantages of short-pulse operation[6] and several of the advantages of steady-state operation,[7] whereas apparently possessing few of the disadvantages of either pulsed or steady operation alone.

This paper presents a series of experimental studies of a parallel-plate accelerator in which current pattern stabilization alone is established and studied, and a series in which both current pattern and gas flow stabilization, i.e., quasi-steady operation, are achieved. These studies are primarily directed toward understanding of some of the basic questions of stabilization phenomena, rather than toward practical implementation. The latter is the subject of a parallel study,[5] however, with which there is considerable interaction.

Presented as Paper 69-112 at the AIAA 7th Aerospace Sciences Meeting, New York, January 20–22, 1969; submitted February 5, 1969; revision received June 3, 1969. This program is supported by NASA Grant NGL 31-001-005.

* Senior Research Scientist. Member AIAA.
† Professor of Aerospace Sciences, Guggenheim Aerospace Propulsion Laboratories. Associate Fellow AIAA.

II. Current Pattern Stabilization

As reported previously,[3] current pattern stabilization first was observed in this laboratory in connection with a series of pulsed exhaust experiments using a linear pinch device that had a large circular orifice in its anode. Stabilization of the current contours projecting out through the orifice occurred when the device was driven with rectangular current pulses of duration greatly in excess of the pinch time of the cylindrical current sheet formed inside the discharge chamber. Similar stabilization of a current sheet at the end of the electrodes of a pulsed coaxial accelerator had been observed elsewhere.[1,2] In order to study this phenomenon in a simpler geometry than any of these, a parallel-plate accelerator, described in detail in Ref. 3, was constructed. Stabilization of the propagating current sheets in this device was achieved by partially insulating the electrode surfaces with thin mylar sheets from a position several inches downstream of the discharge initiation location to the front end of the accelerator (Fig. 1). These initial studies established that spatial stabilization of the propagating current sheets also occurs in this geometry, in the vicinity of the electrode-to-insulator junction.

A more detailed series of diagnostic studies now have been performed using a pair of permanently insulated electrodes.

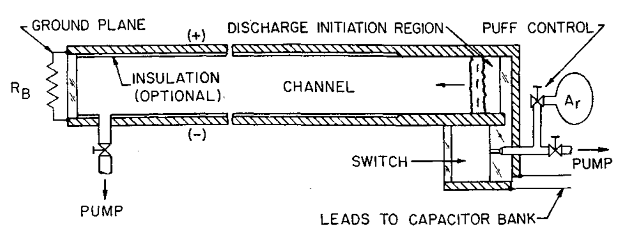

Fig. 1 Schematic diagram of parallel-plate accelerator.

These electrodes consist of $5\frac{1}{4}$-in. lengths of aluminum surface followed by $42\frac{3}{4}$-in. lengths of nylon inlaid insulator surface. The discharge chamber formed by the two electrodes is 48-in. long, 6-in. wide, and has a 2-in. interelectrode spacing maintained by a rectangular Plexiglas housing that forms the side walls of the apparatus. A switch electrode is mounted 2 in. below the bottom electrode in a separate Plexiglas switch chamber. In operation, the switch electrode is connected to a capacitor line charged to -10 *kv*. The top electrode of the accelerator is grounded and the middle electrode also is maintained at ground potential during the charging process by means of a ballast resistor, R_B, connecting the top and middle electrodes. The switch is triggered by injecting argon into its initially evacuated chamber. As the gas pressure increases, the Paschen curve is crossed and the switch discharge initiates, transferring the voltage across the electrodes of the main chamber, resulting in the desired test gas breakdown, sheet formation, propagation, and eventual stabilization processes. The test gas in the main chamber may be set in advance at a given pressure—the ambient mode—or may be injected by a shock tube, a process to be described in detail in connection with the establishment of the quasi-steady mode of operation.

The capacitor line consists of 40×3.2 μF capacitors arranged in various *LC* ladder network configurations to deliver rectangular current pulses ranging from 120,000 *A* for 20 μsec (hereafter designated 120/20), to a nominal 5000 *A* for 500 μsec (5/500).

In the first current pattern stabilization studies to be discussed, the 120/20 pulse is employed and discharged into 100 μ argon, in the ambient mode. Fifty nanosecond Kerr-cell photography is used to view the luminosity associated with various phases of the discharge to indicate its general behavior. The character of the propagating sheet may be seen in Fig. 2, which is a sequence of photographs taken through the side wall normal to the direction of propagation. In these illustrations, Δx is a streamwise coordinate referenced to the metal-to-insulation boundary such that $\Delta x > 0$ is downstream along the insulator, and $\Delta x < 0$ is upstream along the metal electrode portion of the accelerator. The luminous sheet is observed to be nearly one-dimensional at the time of breakdown near the back wall of the chamber, but to become highly two-dimensional as it propagates down the channel. Of interest is the development of a diffuse "anode foot" that enlarges and grows as the sheet propagates. Inception of such a foot has been observed in other experiments of this type[8,9] but here it progresses nearly to the point that it completely dominates the entire luminous pattern, tilting it substantially with respect to the axis and diffusing it over a large dimension.

When the propagating luminous front reaches the end of the exposed electrode, Fig. 3, the luminosity pattern continues to propagate into the insulated channel unrolling, as it were, the stabilized pattern of two broad, nearly axial, and highly luminous bands emanating from the electrode discontinuity. One may speculate that these bright bands are analogous to the anode and cathode jets commonly seen in the magnetoplasmadynamic arcjet.

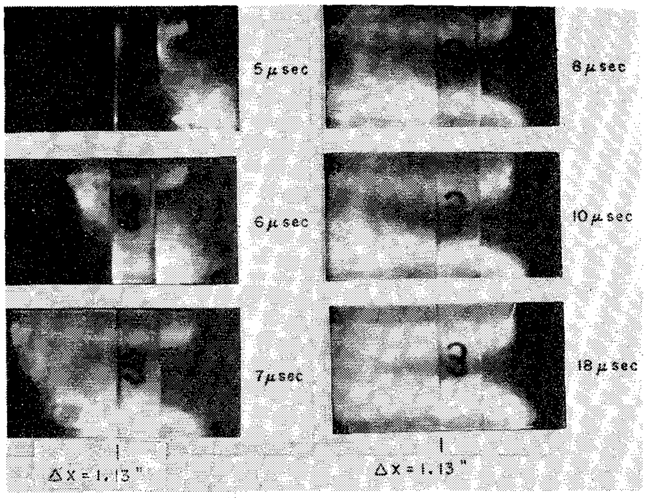

Fig. 3 Transition of discharge to stabilized current distribution.

Confirmation that the current-carrying region has indeed ceased to propagate is best supplied by maps of enclosed current contours at a succession of times, derived from magnetic field probing of the entire discharge column. These maps are displayed in Fig. 4, where the individual contours conform to local current streamlines and their numeral indicates the cumulative current passing everywhere downstream. The slight tilt of the propagating current sheet, its broad anode attachment region and its abrupt arrest at the electrode discontinuity are evident again, in agreement with the luminosity studies. The stabilized pattern bows downstream in a hair-

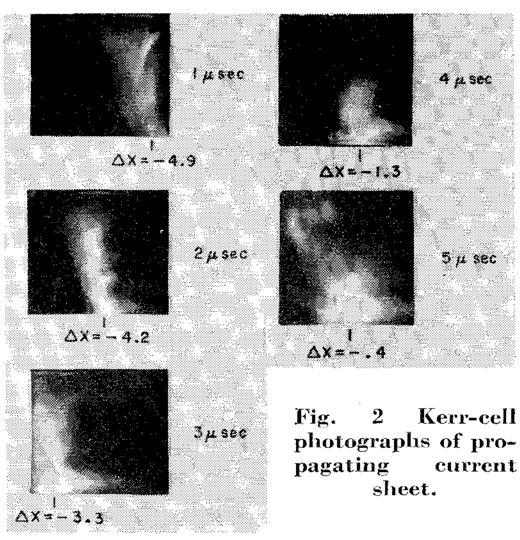

Fig. 2 Kerr-cell photographs of propagating current sheet.

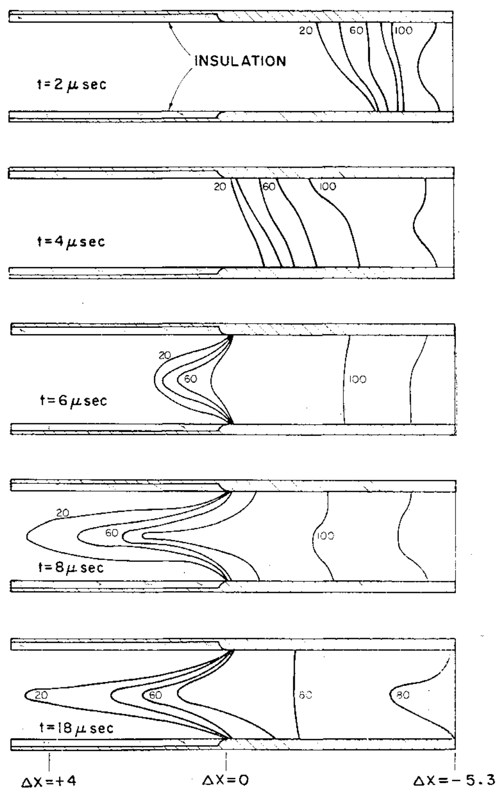

Fig. 4 Enclosed current contours in parallel-plate accelerator (units, 10^3 amp).

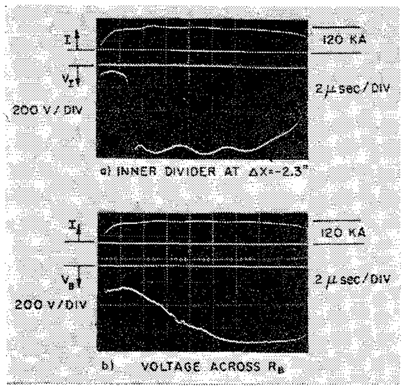

Fig. 5 Voltage signatures of current sheet stabilization.

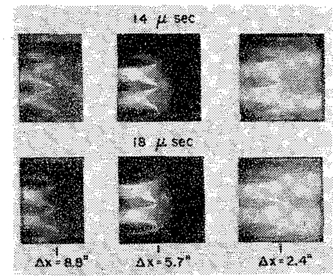

Fig. 7 Airfoil visualization of gas flow through stabilized current distribution.

pin fashion with the bulk of the current conducted across the midplane in the $0 < \Delta x < 6$ in. region, i.e., within three channel heights downstream of the metal-to-insulation junction.

Additional confirmation of current pattern stabilization and valuable indication that the pattern indeed continues to accelerate gas through itself in its stabilized phase is provided by a sequence of terminal voltage measurements made with an inner divider. This device is simply a voltage tap that passes through an insulated port in the anode to electrical contact with the cathode and enables one to separate the resistive and inductive voltage drops in the plasma. Should the current sheet come to rest and start accelerating gas through itself, the probe also will record the corresponding motional emf, regardless of its location. In Fig. 5a the response of the inner divider at $\Delta x = -2\frac{1}{4}$ in., along the metal electrodes, is shown. Before the current sheet sweeps by the probe position, only the resistive drop, here about 60 v, is monitored. This corresponds to a plasma resistance of approximately 0.0005 ohms. As the sheet sweeps by the probing location, the inductance change due to the motion of the sheet is added bringing the total voltage to about 700 v. As the sheet stabilizes, however, this changing inductive contribution should vanish. Note, however, that the voltage signature remains nearly constant. It is hypothesized that the declining flux change contribution is supplemented by the generation of a back emf as the stabilizing current begins to accelerate gas through its self-magnetic field pattern. This hypothesis is verified by monitoring the voltage at the far downstream end of the accelerator where it is impossible to enclose any flux change contribution. The response of the voltage probe at this position is shown in Fig. 5b; initially only the resistive drop is recorded but as stabilization of the current sheet occurs, the back emf contribution also is added.

It thus appears that a new and rather powerful electromagnetic inertial mechanism is operating, i.e., that when the motion of the convecting current sheet is arrested at the electrode discontinuity, the back emf generated in opposition to this change is just sufficient to maintain the terminal voltage at its previous level. The impressive feature of this effect is that the gasdynamic processes involved in its accomplishment are fundamentally quite distinct; that is, there has been a transition from the familiar unsteady mode of gas "sweeping" in a propagating sheet to the equally familiar but rather different steady mode of gas "blowing" though a fixed current pattern, with no observable change in terminal voltage.

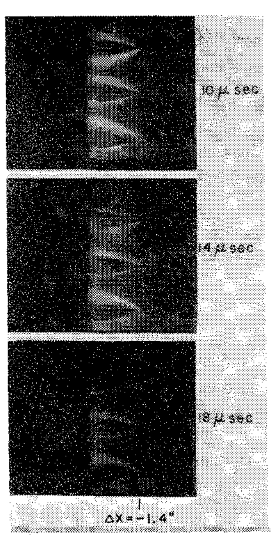

Fig. 6 Airfoil visualization of gas flow into stabilized current distribution.

Although the current has ceased to propagate, acceleration of the gas by the stabilized current distribution appears to continue. The most vivid demonstration of flow acceleration is a photographic sequence of the luminous patterns over small 15° half-angle wedges set in 3 planes, $\frac{1}{4}$ in. off the anode and cathode and in the midplane, at various axial positions along the channel. For example, the state of the inlet flow to the stabilized current zone can be observed by placing the wedges upstream of the current stabilization region, $\Delta x < 0$. Such a series of pictures taken at 10, 14, and 18 μsec, respectively, is shown in Fig. 6 where the wedge tips are located at approximately $\Delta x = -1\frac{3}{8}$ in. Shocks are visible at each of these times indicating that the inflow is supersonic over the stabilized portion of the current pulse. The luminosity of these shocks, however, decreases with time suggesting that the mass flow into the stabilized zone is decreasing. This is to be expected since no external source of mass is available to the discharge.

Figure 7 displays the flow over the wedges at $\Delta x = +2\frac{3}{8}$ in., $+5\frac{5}{8}$ in., and $+8\frac{3}{8}$ in. at 14, 16, and 18 μsec into the pulse. Comparing these positions with the patterns of enclosed current shown in Fig. 4 one sees that the aforementioned positions correspond respectively to the middle of the stabilized zone, to the downstream edge of the zone, and to a completely exterior position. At the three times shown, it is apparent that the Mach number of the flow increases downstream through the stabilized current zone. At the first position, the shocks are somewhat detached; at the second, the shocks are attached, and at the third, they are yet more inclined to the flow. Further interpretation is somewhat ambiguous since either a flow acceleration or a decrease in local sound speed could produce the observed Mach number increase. However, since the effect of joule heating in the current zone would tend to raise rather than lower the sound speed, and since the similarity in probe responses at the three transverse positions speaks against major transverse gradients and excessive wall cooling, a valid flow acceleration through the current zone seems the more likely alternative.

In an effort to unravel a bit more of the mechanisms of gas acceleration in the two phases, the patterns of streamwise and transverse electric field, E_x and E_y, respectively, within the current-carrying region of the plasma are mapped using floating double electric field probes.[10,11] The E_x fields are monitored using a coaxial-lead, conically shaped probe similar to that of Burkhardt and Lovberg. The transverse fields, E_y, are measured with a twisted or coaxial-lead, straight-tipped probe. The streamwise probe response along the metal electrode portion, shown in Fig. 8a, corresponds to that commonly observed for a propagating current sheet,[10,11] namely a "spike" of forward facing electric field. In con-

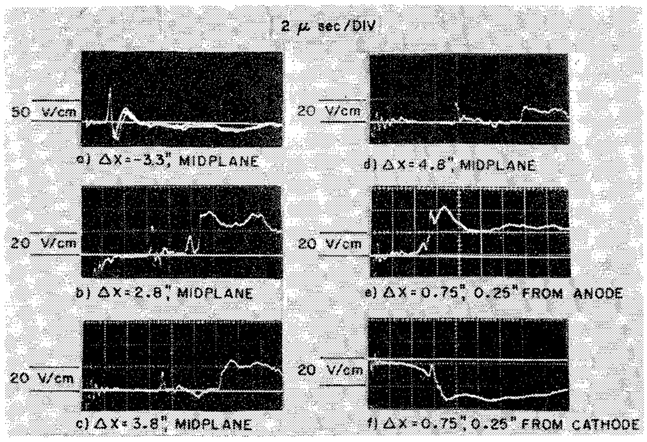

Fig. 8 Streamwise electric field signatures during current sheet stabilization.

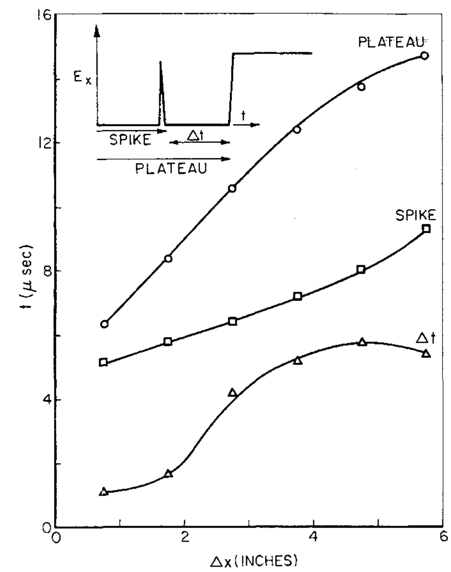

Fig. 9 Trajectories of characteristic features of streamwise electric field signatures.

trast, E_x probe signatures obtained within the stabilized current region, downstream of the metal-to-insulation junction, Figs. 8b, c, and d, consist of a vestige of the current sheet spike followed by a null period, followed by an abrupt rise to a plateau that lasts nearly to the end of the pulse. The amplitudes of the vestigial spike and of the plateau decrease with distance downstream of the electrode discontinuity. The former trends to decelerate beyond the discontinuity but the leading edge of the plateau seems to maintain a uniform speed or even to accelerate somewhat as displayed in the trajectories of Fig. 9.

One may speculate that the first spike of E_x recorded by the probe announces the arrival of the snowplowed plasma accumulated by the propagating sheet upstream in the conducting portion of the accelerator, now continuing on its own inertia as the current sheet is arrested at the discontinuity and diffuses into the stabilized current conduction pattern. The plateau of electric field prevailing over the latter portion of the response presumably reflects the quasi-steady flow acceleration process in operation, possibly as a Hall voltage component of the total electric field. The rather well-defined null time between these two signals is somewhat puzzling, particularly since no correspondingly abrupt processes are evident in the developmemt of the discharge current distribution in this region.

Figures 8e, f display records of E_x obtained by a probe immersed in the conduction bands near the anode and cathode surfaces. Here the E_x field is essentially parallel to the current vector and hence is primarily a resistive component, nearly constant over the lifetime of the steady current pattern and opposite in sign near the anode and cathode. In the stabilized conduction bands, t > 10 μsec, E_y virtually vanishes as seen in Fig. 10a, b.

In Fig. 10c, d, E_y traces along the metal electrodes are shown; these traces rise as the sheet sweeps by and then fall off gradually during the remainder of the pulse. Figure 10e shows the E_y signal in the stabilized zone which, excepting fluctuations, remains relatively constant. The magnitude of E_y in the stabilized zone falls off with distance from the electrode discontinuity going to zero at the end of the stabilized current zone, Fig. 10f.

Magnetic and electric field data like those shown previously can be employed in a simplified, but self-consistent one-dimensional model to yield estimates of the salient properties of the flow passing through the stabilized current zone. Details of this analysis are available in Ref. 4; briefly, it is found that the degree of ionization is about 80%, the outlet to inlet velocity ratio is somewhat greater than 2, and the mass flow rate over the stabilized phase integrates to about 15% of the ambient gas density in the interelectrode gap. The last figure is important in indicating a possible source of mass for the stabilized accelerator, namely gas that has escaped complete entrainment by the propagating current sheet. Current sheets of this intensity, with large anode feet, are known from earlier studies[12] to be "imperfect sweepers" a fact confirmed by the observed magnitude of the E_x spike too small to account for full acceleration of the ions to sheet velocity.

Fig. 10 Transverse electric field signatures.

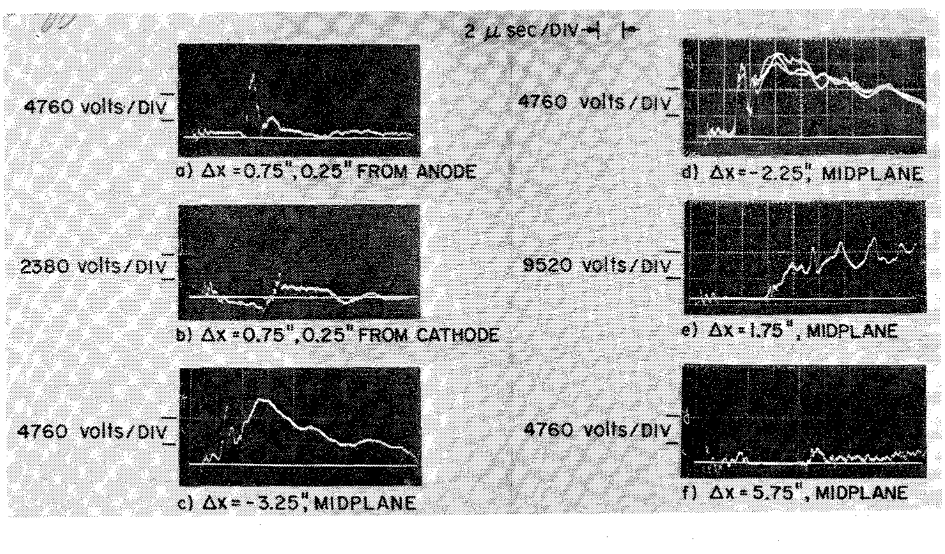

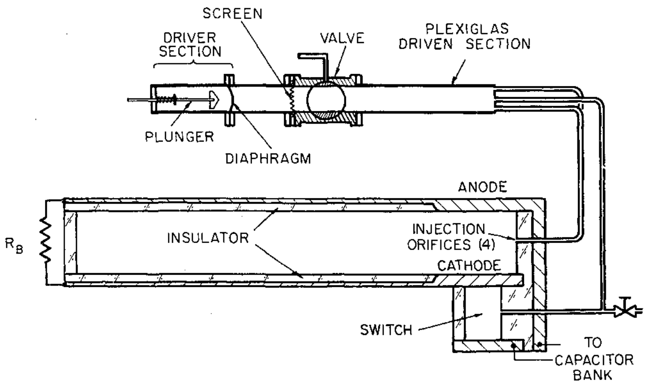

Fig. 11 Shock-tube gas injection system.

Thus, it appears that the propagating sheet only partially accelerates the ambient gas it passes over, which later surges into and is accelerated by the stabilized current pattern.

Clearly this particular source of mass flow can suffice for only a limited time before becoming exhausted. For longer driving pulses, evidence of a decay in this source should appear in the outflow, and such a tendency is indeed observed in wedge flow studies of a 30/80 current pulse.[4] As this supply is depleted, the discharge impedance should rise and/or new sources of mass must be activated. Later in the paper evidence is presented that under these circumstances the discharge increases its voltage to a point where it can ablate sufficient electrode and insulator material to sustain itself on these vapors.

To relieve this mass starvation condition, an external gas supply of some sort is needed, but here one encounters the inherently slow gasdynamic time scale. Figure 11 displays the shock tube gas injection system developed for the parallel-plate accelerator. Despite the substantially superior rise time of such a system over any mechanical gas valve, it is incapable of delivering significant mass to the discharge zone until well over 100 μsec. For example, although discharges driven by 30/80 current pulses show clear evidences of mass starvation toward the end of their flows, no convincing differences in voltage signatures can be observed between discharges in 100 μ ambient argon, and those provided with shock tube gas injection at the same initial pressure. The interpretation is simply that the available time scale (80 μsec) is too short for the injection flow to become properly established. Before the externally supplied gas can provide a quasi-steady inflow to the acceleration zone, it must first fill the channel void created by the sweeping current sheet as

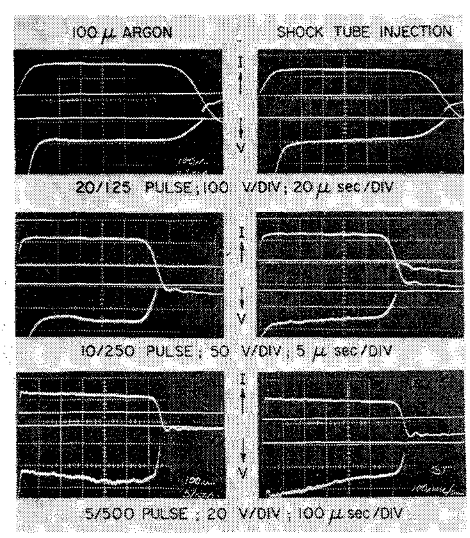

Fig. 12 Voltage signatures indicative of mass starvation.

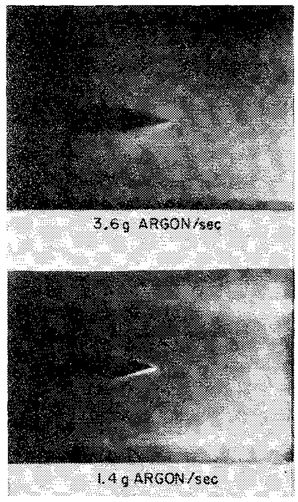

Fig. 13 Kerr-cell phorographs showing increase in anode and cathode jet luminosity with decreasing mass flow.

it propagates to its stabilized position. This filling process must require a time of the order of the channel length involved divided by the sound speed of the injected gas, i.e., hundreds of μsec. In other words, whereas it appears that the electrodynamic aspects of steady plasma acceleration, i.e., current pattern stabilization, can be simulated on a time scale of tens of microseconds, attainment of the corresponding quasi-steady gas flow from an external source will require an order of magnitude longer test time. Experiments directed toward achievement of this quasi-steady mode of plasma acceleration are the subject of the remainder of the paper.

III. Quasi-Steady Plasma Acceleration

Prior to selecting a pulse shape and shock-tube configuration for detailed quasi-steady acceleration experiments, a series of tests was performed to determine the minimum time scale over which the appearance of externally injected gas in the discharge could be established. To reduce the interelectrode cavity upstream of the discharge, the electrodes were shortened from $5\frac{1}{4}$ to 2 in., and downstream terminal voltage signatures were recorded for various current pulse lengths in both the ambient fill and injection modes. Figure 12 compares typical ambient and injection responses for three pulses, 20/125, 10/250, and 5/500. The voltage signatures for the 20/125 pulse in the shock tube and ambient cases are nearly identical, indicating that whereas the shock tube is properly simulating 100 μ initially, it does not succeed in supplying additional mass to the discharge over the balance of the pulse time. For the 10/250 case, however, a difference in the voltage level between the ambient and shock-tube cases can be noticed over the latter half of the pulse. The effect is more evident for the 5/500 pulse where the shape of the entire signature is markedly different, and near the end of the pulse the shock-tube voltage is nearly 50% lower than the ambient value. It seems qualitatively reasonable that the ambient signals should increase with time due to a mass starvation of the discharge, while the shock tube signatures decrease as the injected flow increases the pressure in the discharge region. Based on a series of such studies, it is concluded that an externally supplied gas flow from the existing shock tube injection system can be established at the discharge region for pulse times of 150 μsec or greater.

To verify that the external flow, which on the basis of the voltage measurements appears to be feeding the discharge, is indeed being accelerated, a small 15° half-angle wedge again is placed $2\frac{1}{4}$ in. downstream of the metal-to-insulation discontinuity, hopefully to generate visible bow shocks. Now, however, for the relatively low-discharge current amplitudes predicated by the long pulse requirement, the flow luminosities are much less intense, and this technique becomes marginal, at best. For the 5/500 pulse, the luminosity of the flow is too weak to be photographed even with a 5 μsec Kerr-cell shutter. For the 10/250 waveform, visible bow shocks are found, but only for a narrow range of injected mass flow rate of the order of 3.5 gm/sec, as determined by sensitive piezo transducers and a simple volume filling procedure.

In this particular range of mass flow, however, the desired effect has been demonstrated; namely, the device has succeeded in accomplishing the transitions from its initial transient phase, through an interim phase where it accelerates overrun ambient gas and/or electrode-insulator material, to the quasi-steady phase where it accelerates an externally injected gas flow. To examine this latter phase in more detail, a series of electric and magnetic probe studies again have been performed to map the prevailing field, and current distributions. Details of this work, and of the analysis based on it are available in Ref. 4; briefly, it is found that unlike the high-current patterns, which are bowed far downstream, the 10/250 current distribution is nearly one-dimensional, and the streamwise electric field falls to zero upstream of the current density maximum. The analysis then indicates a velocity ratio of about 2.5 across the acceleration zone, and a degree of ionization of about 20% within it.

One interesting by-product of the otherwise meager Kerr-cell results of the long pulse discharges has been the revelation of greatly increased luminosity in the anode and cathode jets emanating from the electrode-insulator discontinuities as the mass flow decreases (Fig. 13). It is hypothesized that as the mass flow decreases, the discharge is starved for mass and ablates electrode and/or insulator material to feed itself, with a resulting intensification of the luminosity near the electrode discontinuity. To check this hypothesis, the discharge has been examined spectroscopically for the various mass flow rates available. As the external flow is reduced, there is observed to be a major increase in the intensity of the molecular carbon bands, an increase in the intensity of aluminum lines, and a decrease in the argon line radiation.[4] If one associates the carbon with the organic insulator material, the hypothesis seems at least qualitatively confirmed.

IV. Summary

Based on the experiments described in this paper, detailed analyses developed in another reference,[4] and earlier work,[3] we may piece together the following picture of the metamorphosis of the plasma acceleration process in the parallel-plate, partial-electrode channel driven by a long current pulse: At breakdown a current sheet is formed near the upstream end of the electrode channel, of width and intensity determined by the rise time and amplitude of the driving pulse. Driven by its own magnetic field, this sheet propagates into the ambient gas, entraining a large fraction of it, but leaving some profile of slower gas in its wake. Upon reaching the electrode-insulator discontinuity, the sheet decelerates rapidly to a stabilized discharge configuration, while the gas entrained on it continues down the channel on its own inertia. The stabilized discharge, whose particular configuration again depends on the amplitude of the driving current, now is fed from the upstream side by the slower gas left behind the current sheet, which gas it accelerates through itself in the classical self-field Lorentz mode to a velocity that maintains the terminal voltage the same as the transient-phase value. In the absence of another source of mass, the discharge eventually exhausts this reservoir of overswept gas, and begins to vaporize insulator and/or electrode material to maintain itself, much like a "vacuum arc." This phase is characterized by increased luminosity of the anode and cathode jets, and an increase in arc voltage. If an external mass source is provided, this must first refill the channel upstream of the stabilized discharge before any quasi-steady inlet flow to the discharge region can be established. This is a relatively slow process, and depending on particular channel dimensions and injection procedures, may take 100 μsec or more. Once such inlet flow is established, however, the discharge voltage drops, erosion luminosity is sharply reduced, and the accelerator operates on the injected mass flow in the same quasi-steady, self-field mode.

References

[1] Gorowitz, B., Gloersen, P., and Karras, T., "Study of Parametric Performance of a Two-Stage Repetitively Pulsed Plasma Engine (REPPAC)" Summary Report NASw-1044, CR-54846, March 31, 1966, NASA.

[2] Ashby, D. E. T. F. et al., "Development of a Coaxial Plasma Gun for Space Propulsion," NASA Contract NAS 3-5759, CR-54245, April 1965, Convair/General Dynamics Corp., San Diego, Calif.

[3] Eckbreth, A. C., Clark, K. E., and Jahn, R. G., "Current Pattern Stabilization in Pulsed Plasma Accelerators," *AIAA Journal*, Vol. 6, No. 11, Nov. 1968, pp. 2125–2132.

[4] Eckbreth, A. C., "Current Pattern and Gas Flow Stabilization in Pulsed Plasma Accelerators," Ph.D. thesis, Dec. 1968, Princeton Univ., Princeton, N. J.

[5] Clark, K. E., "Quasi-Steady Plasma Acceleration," Ph.D. thesis, May 1969, Princeton Univ., Princeton, N. J.

[6] Jahn, R. G., *The Physics of Electric Propulsion*, McGraw-Hill, New York, 1968.

[7] Ashby, D. E. T. F., Liebing, L., and Larson, A. V., "Quasi-Steady State Pulsed Plasma Thrusters," *AIAA Journal*, Vol. 3, No. 6, June 1965, pp. 1209–1210.

[8] MacLelland, J. R., MacKenzie, A. S., and Irving, J., "Schlieren Photography of Rail Tube Plasmas," *The Physics of Fluids*, Vol. 9, No. 8, Aug. 1966, p. 1613.

[9] Liebing, L., "Motion and Structure of a Plasma Produced in a Rail Spark Gap," *The Physics of Fluids*, Vol. 6, No. 7, July 1963, p. 1035.

[10] Burkhardt, L. C. and Lovberg, R. H., "Current Sheet in a Coaxial Gun," *The Physics of Fluids*, Vol. 5, No. 3, March 1962, p. 341.

[11] Burton, R. L., "Structure of the Current Sheet in a Pinch Discharge," Ph.D. thesis, Sept. 1966, Princeton Univ., Princeton, N. J.

[12] Ellis, W. R., Jr., "An Investigation of the Current Sheet in a Cylindrical Z-Pinch," Ph.D. thesis, July 1967, Princeton Univ., Princeton, N. J.; Ellis, W. R., Jr. and Jahn, R. G., "Ion Density and Current Distributors in a Propagating Current Sheet, Determined by Microwave Reflection Technique," *Journal of Plasma Physics*, Vol. 3, Pt. 2, 1969, p. 189.